Phonon Transport of Rough Si/Ge Superlattice Nanotubes

Yuhang Jing[1] and Ming Hu[2,3]

Abstract: Nanostructuring of thermoelectric materials bears promise for manipulating physical parameters to improve the energy conversion efficiency of thermoelectrics. In this paper the thermal transport in Si/Ge superlattice nanotubes is investigated by performing nonequilibrium molecular dynamics simulations aiming at realizing low thermal conductivity by surface roughening. Our calculations revealed that the thermal conductivity of Si/Ge superlattice nanotubes depends nonmonotonically on periodic length and increases as the wall thickness increases. However, the thermal conductivity is not sensitive to the inner diameters due to the strong surface scattering at thin wall thickness. In addition, introducing roughness onto the superlattice nanotubes surface can destroy the phonon tunneling in superlattice nanotubes, which results in thermal conductivity even surpassing amorphous limit. Furthermore, a nonmonotonic dependence of the thermal conductivity of rough Si/Ge superlattice nanotubes with thicker wall thickness is found, while for thinner wall the thermal conductivity of rough Si/Ge superlattice nanotubes decreases monotonically with surface roughness increasing. Our results provide guidance for designing high performance thermoelectrics using superlattice nanotube.

Keywords: Si/Ge superlattice nanotubes, thermal conductivity, surface roughness, nanoscale heat transfer, molecular dynamics simulation.

1 Introduction

One-dimensional silicon nanostructures have attracted significant attention due to their tremendous technological potential in nanoscale devices [Morales and Lieber

[1] Department of Astronautical Science and Mechanics, Harbin Institute of Technology, Harbin 150001, China.

[2] Institute of Mineral Engineering, Division of Materials Science and Engineering, Faculty of Georesources and Materials Engineering, RWTH Aachen University, 52064 Aachen, Germany. Author to whom all correspondence should be addressed. E-Mail: hum@ghi.rwth-aachen.de (M.H.)

[3] Aachen Institute of Advanced Study in Computational Engineering Science (AICES), RWTH Aachen University, 52062 Aachen, Germany.

(1998); Lieber (2002)] and compatibility with conventional Si-based electronic technology [Huang, Duan Cui Lauhon Kim and Lieber (2001)]. Single crystalline silicon nanowires (NWs) have been synthesized successfully by various synthetic methods [Holmes Johnston Doty and Korgel (2000); Zhang Tang Wang Yu Lee Bello and Lee (1998); Wang Zhang Tang Lee and Lee (1998); Wu Cui Huynh Barrelet Bell and Lieber (2004); Kikkawa Ohno and Takeda (2005)]. Many possible applications of Si NWs, especially as field-effect transistors or optical and photonic devices, have already been reported [Cui and Lieber (2001); Zheng, Lu, Jin and Lieber (2004); Guiksen, Lauhon, Wang, Smith and Lieber (2002)]. In addition to their electronic properties, thermal transport properties of Si NWs are also of great interest for fundamental physics and potential applications, especially when Si NWs are used as thermoelectric materials. Recently, experimental and theoretical investigations have demonstrated that Si-based NWs have very low thermal conductivity compared to that of bulk silicon, which makes Si NW a good candidate for thermoelectric materials [Hochbaum, Chen, Delgado, Liang, Garnett, Najarian, Majumdar and Yang (2008); Donadio and Galli (2009); Hu, Giapis, Goicochea, Zhang and Poulikakos (2011)]. The energy conversion efficiency of thermoelectric devices is characterized by the figure-of-merit: $ZT = S^2 \sigma T / \kappa$, where S, σ, T, and κ are the Seebeck coefficient, electrical conductivity, absolute temperature, and thermal conductivity of the material, respectively. The engineering of nanostructured materials with very low thermal conductivity is a necessary step toward the realization of efficient thermoelectric devices. In context of reducing thermal conductivity, Si/Ge core/shell nanowires (CSNW) [Hu, Giapis, Goicochea, Zhang and Poulikakos (2011); Hu, Zhang, Giapis and Poulikakos (2011); Zhang, Hu, Giapis and Poulikakos (2012); Lauhon, Gudiksen, Wang and Lieber (2002)] and Si/Ge superlattice nanowire (SLNW) [Li, Wu, Fan, Yang and Majumdar (2003); Chakraborty, Kleint, Heinrich, Schneider, Schumann, Falke and Teichert (2003); Liu, Yu, Chien, Kuo, Hsu, Dai, Luo, Huang and Huang (2008); Hu and Poulikakos (2012)] attracted great attention due to the strong interfacial phonon scattering that significantly reduces the thermal conductivity and thus can potentially improve *ZT* coefficient. However, it was demonstrated that there are two competing mechanisms governing the thermal transport in Si/Ge superlattice nanowires [Hu and Poulikakos (2012)]: interface modulation and coherent phonons, responsible for hindering heat conduction and facilitating thermal transport, respectively. Due to the presence of coherent phonons, the thermal conductivity of Si/Ge SLNW cannot be reduced further as periodic length becomes extremely short. This poses a substantial barrier against maximizing *ZT* values of SLNWs as a potential effecient thermoelectric material.

Comparing with filled Si NWs, hollow silicon nanotubes (NTs) induce more sur-

face phonon scattering [Chen, Zhang and Li (2010)]. By consistently drilling a small hole at the center of thin (cross section of 2.72×2.72 nm) Si NWs to form a nanotube, their simulations suggest that a 1% reduction in the NW cross section can cause a 35% reduction in room-temperature thermal conductivity. [Chen, Zhang and Li (2010)]. Now an intuitive idea is to combine the concept of superlattice nanowire [Hu and Poulikakos (2012)] and hollow nanotube. We call it superlattice nanotube (SLNT). That is to say, instead of filled superlattice nanowire, we remove the central part to form a superlattice nanotube. In this paper, we construct a serial of Si/Ge SLNTs and investigate the phonon transport in Si/Ge SLNTs using nonequilibrium molecular dynamics (NEMD) simulations. The effects of periodic length, thickness, cross section area (diameter of the SLNT), and surface morphology (roughness) on thermal conductivity are explicitly considered. In particular we introduce roughness onto the SLNT surface and expect to destroy the coherent phonons in SLNT, such that the thermal conductivity can be further reduced.

2 Model structures and simulation methodology

Our model structure consists of Si/Ge superlattice nanotube oriented (extended) in [111] direction. The cross-sectional views of the circular SLNTs are shown in Fig. 1. The longitudinal direction is set along the *y*-axis, i.e. the direction of heat flow. The inner diameter of the nanotube is 2.1 nm with wall thicknesses of 1.1, 2.4, and 3.8 nm, respectively. In addition, we also construct nanotubes with similar thickness but different inner diameters. The thickness of the nanotube is 1.1 nm with inner diameters of 2.1, 4.1, and 8.3 nm, respectively. The SLNTs consist of alternating Si and Ge layers with periodic lengths ranging from 0.66 nm to 15.7 nm. An overview of a typical SLNT structure is shown in Fig. 2. All nanotubes have the same total length of 77 nm. The average lattice constant of 0.554 nm for Si and Ge is used to construct initial structure of SLNTs. In all MD simulations performed herein, the Tersoff potential with original parameters optimized for Si-Ge systems is used to describe the interactions between Si and Si atoms, Ge and Ge atoms, and Si and Ge atoms in Si/Ge SLNTs. This potential has been widely employed to study the thermal transport properties of Si nanowire with amorphous layer [Donadio and Galli (2010)], nanoporous Si-Ge [He, Donadio and Galli (2011)], Si-Ge quantum dot superlattices [Haskins, Kinaci and Cagin (2011)], and Si/Ge superlattice NWs [Hu and Poulikakos (2012)].

All MD simulations are performed using LAMMPS package [Plimpton (1995)].The Velocity-Verlet algorithm is employed to integrate the equations of motion with a timestep of 0.55 fs. All molecular systems were equilibrated at a constant pressure of 1 atm and a temperature of 300 K using *NPT* (constant number of particles, pressure, and temperature) for 100 ps. The temperature is controlled by employing the
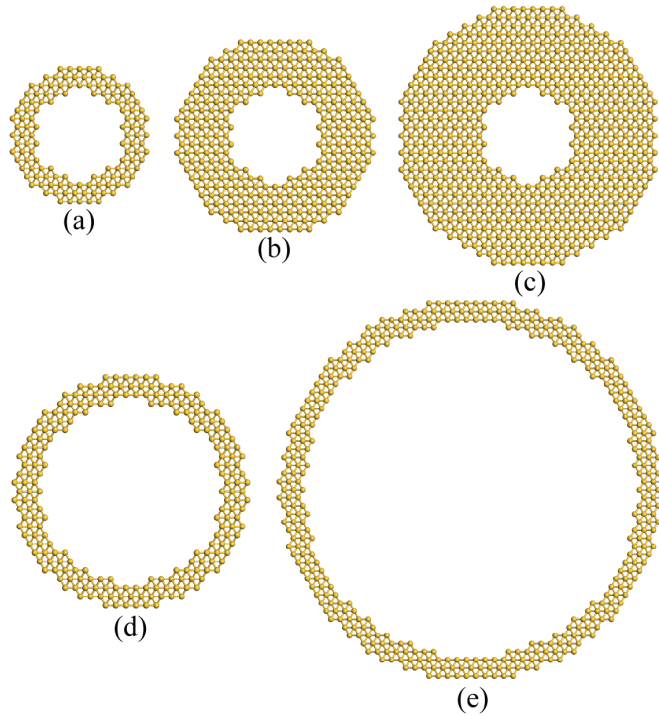
Figure 1: Cross section views of the [111]-oriented Si/Ge SLNTs. Top panel: The inner diameter of the nanotube is 2.1 nm with wall thickness of (a) 1.1,(b) 2.4, and (c) 3.8nm. Bottom panel: The thickness of the nanotube is 1.1 nm with inner diameter of (d) 4.1 and (e) 8.3 nm.

Nosé-Hoover thermostat [Hoover (1985)]. After the *NPT* relaxation, we continued to relax the system with an *NVE* (constant volume and no thermostat) ensemble for 100 ps. During this stage, we monitored the total energy and temperature of the entire system. We found that the total energy conserved very well and the temperature remained constant with small fluctuations around 300 K, which meant that the system had reached the equilibrium state.

Following equilibration, we compute the thermal conductivity of the structures using nonequilibrium molecular dynamics (NEMD). The constant heat flux is imposed by the Muller-Plathe method [Muller-Plathe (1997)]. During the NEMD simulation process, the simulation domain is divided into slices along the longitudinal (*y*-) direction. The outmost two layers on the nanotube ends are defined as "hot slab" and "cold slab", respectively. The coldest atoms in the "hot slab" and the hottest atoms in the "cold slab" are selected and their kinetic energies are ex-
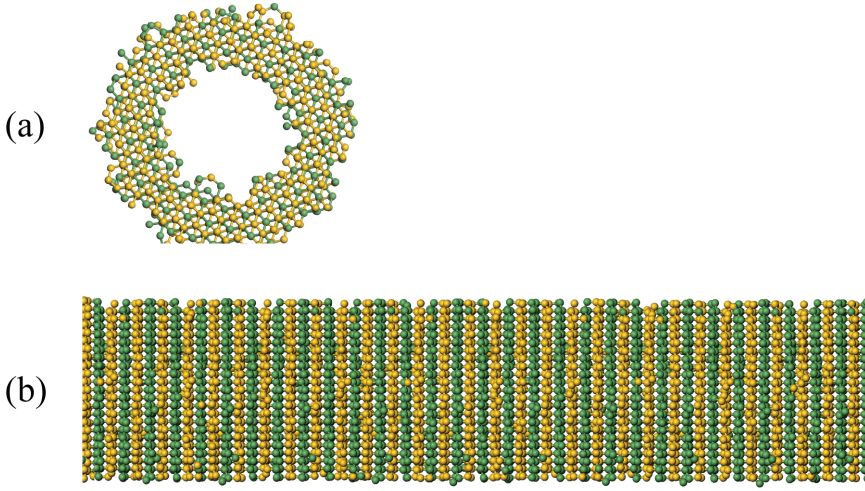
Figure 2: Overview of a typical Si/Ge superlattice nanotube used as model system in the MD simulations. The total length of the SLNT is 77 nm with inner diameter 2.1 nm, shell thickness 2.4 nm, surface roughness concentration 50%, and periodic length 0.66 nm. Color code: yellow: Si, cyan: Ge.

changed every few time steps. This operation will introduce a constant heat flux into the system and also there will be a temperature gradient after running some time. The thermal conductivity is calculated by the Fourier's law

$$\kappa = -\frac{J_L}{\partial T/\partial z},$$ (1)

where J_L is the averaged heat flux in the longitudinal direction and $\partial T/\partial z$ is the temperature gradient determined from the linear fitting to the temperatura profile. Once the steady state is reached, which typically takes $1-3$ ns depending on the system, we run additional 5 ns to collect data for averaging heat flux and temperature gradient.

3 Simulation results and discussion

3.1 Thermal conductivity dependence of periodic length, wall thickness, and diameter

The thermal conductivity of Si/Ge SLNTs as a function of SL periods for three nanotube wall thickness is shown in Fig. 3. The inner diameter of the nanotube
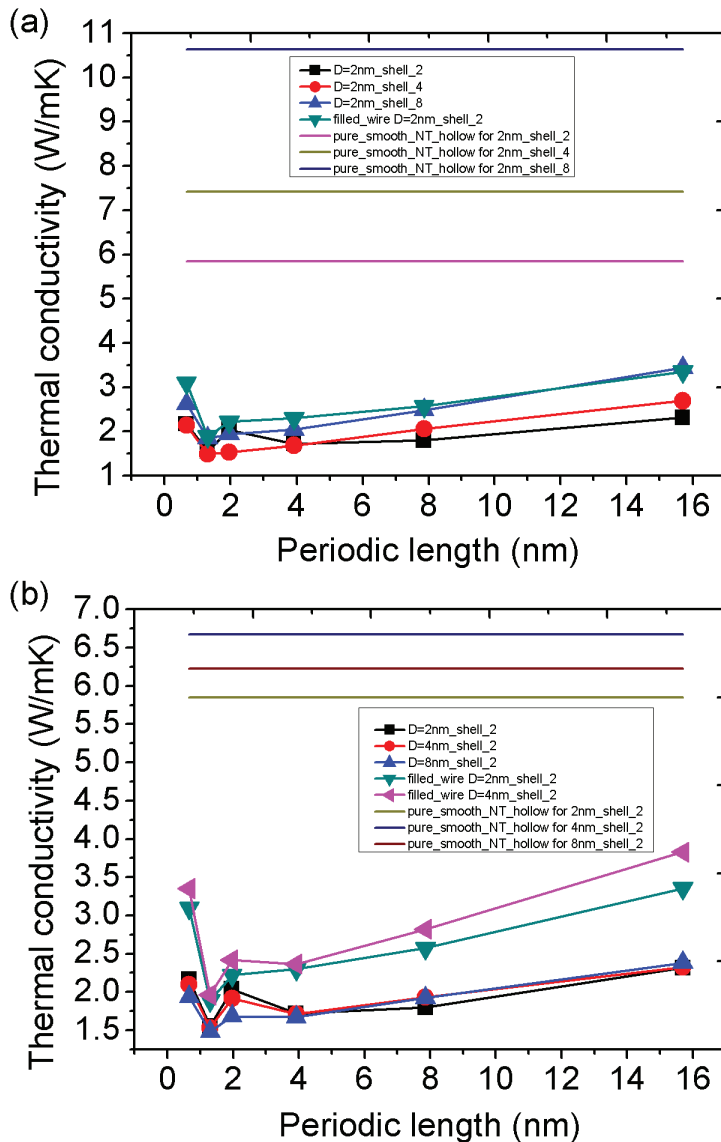
Figure 3: Dependence of thermal conductivity of Si/Ge SLNTs on periodic length. (a) SLNTs with different wall thicknesses; (b) SLNTs with different inner diameters. For comparison pure smooth hollow Si NTs with same cross-sectional area are also included (horizontal lines).

is 2.1 nm with wall thickness of 1.1, 2.4, and 3.8 nm, which are depicted in Fig. 3 as "D=2nm_shell_2", "D=2nm_shell_4", and "D=2nm_shell_8", respectively. The thickness of the nanotube is 1.1 nm with inner diameter of 4.1 and 8.3 nm, which are depicted in Fig. 3 as "D=4nm_shell_2" and "D=8nm_shell_2", respectively. The cross sections of the nanotube are shown in Fig. 1. Results for pure smooth hollow Si NTs and Si/Ge SLNWs with same cross-sectional area are also included in Fig. 3 for comparison. The "filled_wire D=2nm_shell_2" and "filled_wire D=4nm_shell_2" mean the filled Si/Ge superlattice nanowire with the same cross-sectional area to the Si/Ge SLNT with wall thickness of 1.1 nm and inner diameters of 2.1 and 4.1 nm, respectively. Similar to the previous simulations and experiments [Hu and Poulikakos (2012); Simkin and Mahan (2000); Venkatasubramanian (2000); Lin and Strachan (2013)], the nonmonotonic dependence of the thermal conductivity of Si/Ge SLNWs on the periodic length is found, which validates our results. The similar trends for Si/Ge SLNTs are also observed and a minimum thermal conductivity for the SLNTs with certain periods is obtained in our results. The minimum occurs at periodic length of about 1.3 nm for all superlattice nanotubes. We can notice from Fig. 3 that the thermal conductivity of Si/Ge SLNTs is remarkably reduced as compared to that of pure smooth Si nanotubes. For example, the reduction percentage in thermal conductivity reaches as high as 73%, 79%, and 82% for the superlattice nanotubes with inner diameter 2.1 nm and wall thickness of 1.1, 2.4, and 3.8 nm, respectively. We also notice that the thermal conductivity of Si/Ge SLNTs increases as the wall thickness of nanotubes increases. This can be attributed to the increased area of single crystalline structure which contributes largely to the overall thermal transport. However, as shown in Fig. 3(b), the thermal conductivity of Si/Ge SLNTs is not sensitive to the inner diameters due to the strong surface scattering at thin wall thickness.

3.2   *Mechanism: phonon polarization analysis*

In order to study the origin of such interesting phenomena, we first perform phonon polarization analysis to the molecular system. To this end, we followed the method we proposed recently [Hu, Zhang and Poulikakos (2013); Zhang, Hu and Tang (2013)] to quantify the relative contributions of longitudinal, transverse, and flexural modes to the total phonon transport. We define an imaginary cross-section normal to the longitudinal direction (x), set there the coordinate origin $x = 0$, and denote the atoms on the two sides of this origin as "left", respectively "right". Then the contribution to the total heat flux in the SLNT due to the vibration in a specific direction can be expressed as [Hu, Zhang and Poulikakos (2013); Zhang, Hu and

Tang (2013)]

$$J_{left \to right,\alpha} = -\frac{1}{2S} \sum_{i \in left} \sum_{j \in right} F_{ij\alpha}(v_{i\alpha} + v_{j\alpha}) \tag{2}$$
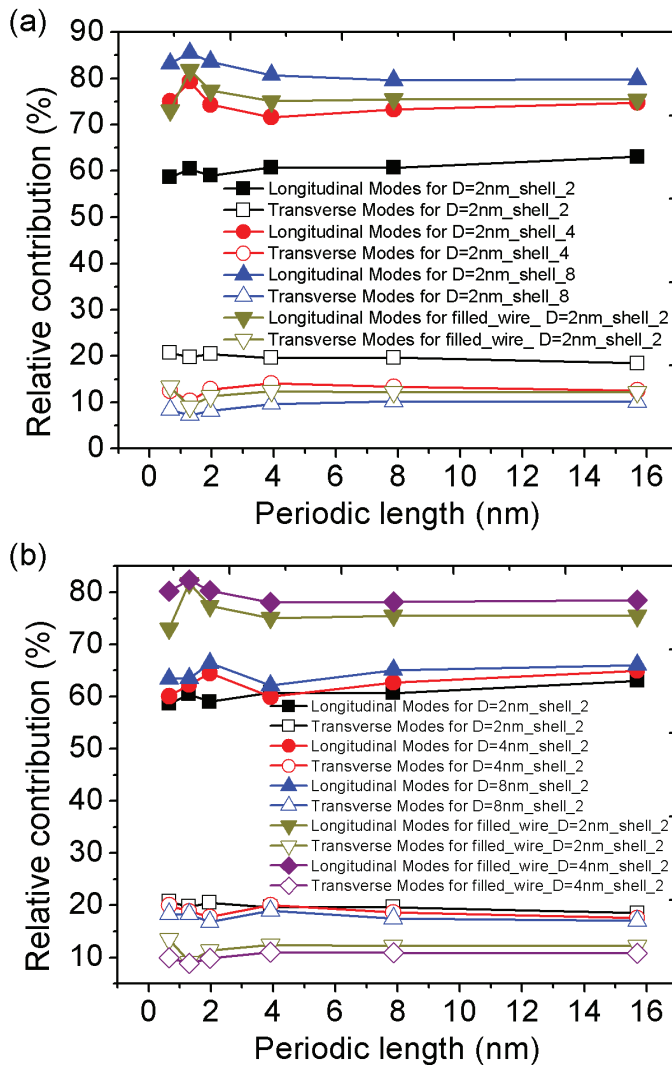

Figure 4: Relative contribution (percentage) to total heat flux from vibrations in longitudinal and transverse directions as a function of periodic length of SLNTs. (a) SLNTs with different wall thicknesses; (b) SLNTs with different inner diameter.

where $J_{left \to right, \alpha}$ is the heat flux across the imaginary interface contributed by the lattice vibrations in the α direction, α can be the x, y, or z direction, S is the cross-sectional area of the nanotube, $F_{ij\alpha}$ is the α-component of the force acting on atom i due to atom j, $v_{i\alpha}$ is the α-component of the velocity of atom i, and the two sums are taken over atoms i and j belonging to the group of "left" and "right", respectively. Note that the above formula is based on two-body interactions, but the Tersoff potential used is a three-body potential. To calculate the results of equation above, we decompose the three-body forces into two-body components. For example, assume that atoms i, j, and k are the three bodies in interaction, then the force $\vec{F}_i$ can be decomposed to be $\vec{F}_{ij}$ and $\vec{F}_{ik}$, which can be considered as the forces acting on atom i due to atom j and atom k, respectively. Similar treatment can be applied to the forces of $\vec{F}_j$ and $\vec{F}_k$. For all cases, we have verified that the sum of the three components of the heat fluxes calculated by Eq. (2) is technically equal to J_L in Eq. (1) after very long time averaging (typically at least longer than 2500 ps). Fig. 4 shows the relative contribution to the total heat flux from the vibrations in longitudinal and transverse directions as a function of periodic length of SLNTs for different wall thicknesses and inner diameters. For SLNTs with different wall thicknesses, the relative contribution of longitudinal modes increases as the nanotube wall thickness increases, as shown in Fig. 4(a). However, the relative contribution of longitudinal modes of SLNTs is not sensitive to inner diameter, as shown in Fig. 4(b). The trend of the longitudinal mode contribution with the change of nanotube wall thickness and inner diameter is consistent with the trend found in the wall thickness dependence and inner diameter independence of the thermal conductivity of the SLNTs presented in Fig. 3. In addition, the thermal conductivity of Si/Ge SLNT is always lower than that of Si/Ge SLNW for all periodic lengths, which makes Si/Ge SLNT a very promising nanomaterial for high efficiency thermoelectrics.

3.3 Effect of surface roughness on phonon transport

However, Fig. 3 also clearly shows that the thermal conductivity of Si/Ge SLNT cannot be reduced further as periodic length becomes extremely short, which poses a substantial barrier against maximizing *ZT* values of SLNT as a potential effecient thermoelectric material. To overcome this, we introduce roughness onto the SLNT surface and expect to destroy the phonon tunneling in SLNT, such that the thermal conductivity can be further reduced. Fig. 5 shows the periodic length dependence of the thermal conductivity of Si/Ge SLNTs with different surface roughness. We first notice that the thermal conductivity of Si/Ge SLNTs decreases as the roughness increases, which is consistent with the previous studies of edge roughness on the thermal conductivity of silicon nanowires [Donadio and Galli (2009); Liu and Chen

(2010)]. This indicates that phonon scattering due to the surface roughness will further reduce the thermal conductivity of nanostructures. The most significant result in Fig. 5 is that the thermal conductivity of the Si/Ge SLNTs is reduced further as periodic length becomes extremely short. That is to say, the surface roughness successfully destroys the phonon tunneling in SLNT. For example, as the periodic length reaches 0.66 nm, compared with pure smooth Si nanotubes, the reduction percentage in thermal conductivity of Si/Ge SLNT with inner diameter 2.1 nm and wall thickness of 2.4 nm reaches as high as 82%, 85%, and 87% for surface roughness of 10%, 20% and 30%, respectively.

In order to study the physical mechanism of the reduction of the thermal conductivity, we also studied the relative contribution (percentage) to total heat flux from vibrations in longitudinal and transverse directions as a function of periodic length of SLNTs with inner diameter of 2.1 nm and wall thickness of 2.4 nm, as shown in Fig. 6. At the shortest periodic length, the relative contribution of longitudinal modes decreases as the surface roughness increases. In other words, the relative contribution of transverse modes increases with the increasing of the surface roughness. Thus, the lower frequency and wave velocity of the transverse modes will result in a lower thermal conductivity. More evidence is provided by the vibrational density of states (VDOS) of interior atoms in Fig. 7. As the surface roughness increases, the VDOS moves towards lower frequency. Specifically, the low frequency parts (below 3.5 THz) of the VDOS of the SLNTs are increased. That is to say, the transverse modes are enhanced, which leads to the reduction of thermal conductivity.

From the above results and discussions we know that the thermal conductivity of the SLNTs can be strongly affected by the surface roughness. An intuitive motivation is to systematically study the effect of the surface roughness on the phonon transport in the Si/Ge SLNTs. Fig. 8 shows the thermal conductivity of Si/Ge SLNTs as a function of surface vacancy concentration (surface roughness).The periodic length of Si/Ge/ SLNTs is 0.66 nm. The results for amorphous Si NW and Si/Ge NW are also shown in Fig. 8 for comparison. It is interesting to notice that for the two different Si/Ge SLNTs the trends are different. For the Si/Ge SLNTs with the inner diameter of 2.1 nm and wall thickness of 2.4 nm, a nonmonotonic dependence is found. The lowest thermal conductivity is only 42% of that of the Si/Ge SLNTs without surface roughness, which occurs at the surface roughness of 50%, and the thermal conductivity of Si/Ge SLNTs increases as the surface roughness increases further. This can be understood that, when the surface roughness is 100%, a smooth Si/Ge SLNT with smaller diameter will form. It is worth pointing out that when we calculate thermal conductivity of SLNTs with rough surfaces, we assume the cross-sectional area decreases linearly as surface roughness concentration changes
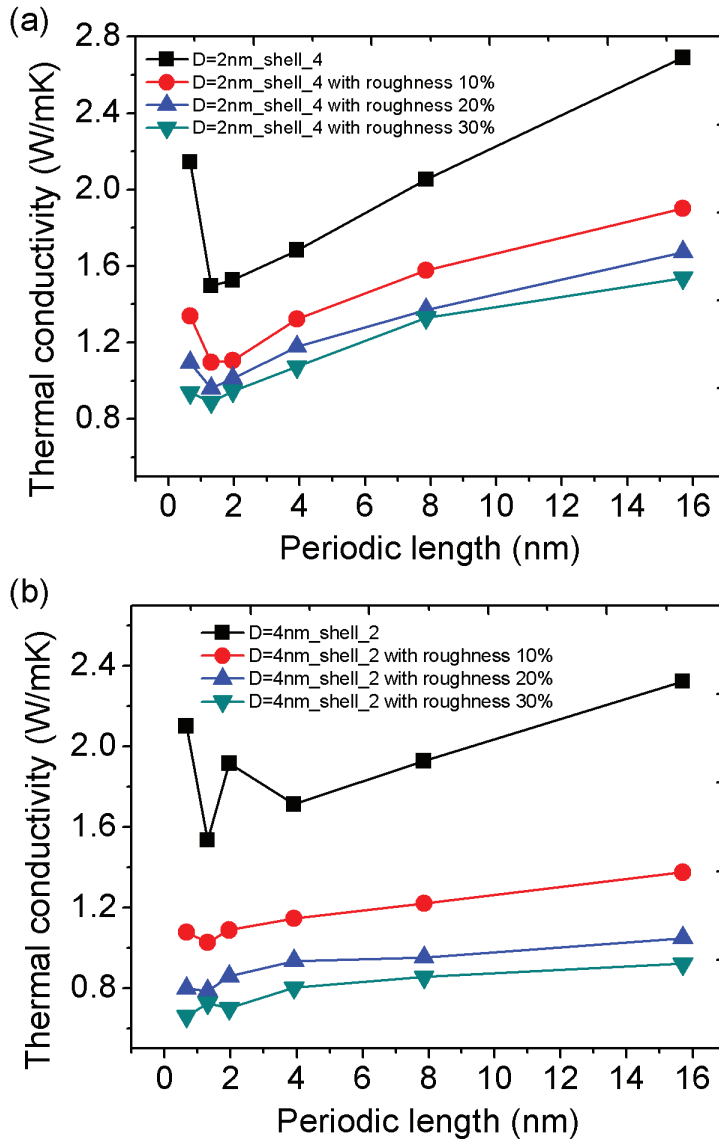
Figure 5: Periodic length dependence of the thermal conductivity of Si/Ge SLNTs with different surface roughness. (a) The inner diameter of the nanotube is 2.1 nm with wall thickness of 2.4 nm. (b) The thickness of the nanotube is 1.1 nm with inner diameter of 4.1 nm.
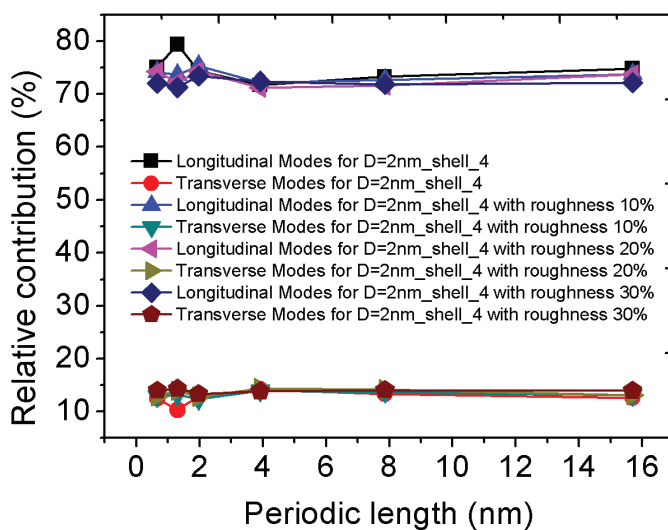
Figure 6: Relative contribution (percentage) to total heat flux from vibrations in longitudinal and transverse directions as a function of periodic length of SLNTs with different surface roughness.

from 0% to 100%. Therefore, when the surface roughness is larger than 50%, the whole structure can be considered as a relatively thinner smooth Si/Ge SLNT covered with some protuberant rough dots on the surface. When the surface roughness is smaller than 50%, the whole structure can be considered as a relatively thicker smooth Si/Ge SLNT with some voids on the surface. We also notice from Fig. 8 that the thermal conductivity of Si/Ge SLNTs with surface roughness is smaller than that of pure amorphous Si nanowire with same cross-sectional area to Si/Ge SLNT (D=2nm_shell_4) with 50% surface roughness, indicating again that introducing roughness onto the SLNT surface is efficient to reduce the thermal conductivity. In addition, the thermal conductivity of Si/Ge SLNTs with surface roughness approaches that of amorphous $Si_{0.5}Ge_{0.5}$ alloy nanowire with same cross-sectional area to Si/Ge SLNT (D=2nm_shell_4) with 50% surface roughness. However, for the Si/Ge SLNTs with the inner diameter of 4.1 nm and wall thickness of 1.1 nm, the thermal conductivity of Si/Ge SLNTs depends monotonically on the surface roughness and even goes below the amorphous limit of $Si_{0.5}Ge_{0.5}$ alloy nanowire. As the surface roughness increases, the thermal conductivity decreases, as the wall thickness is very small in this case such that phonon scattering strongly affects thermal transport. Actually we observed that the structure becomes more or less amorphous like as the surface roughness concentration reaches 70%.
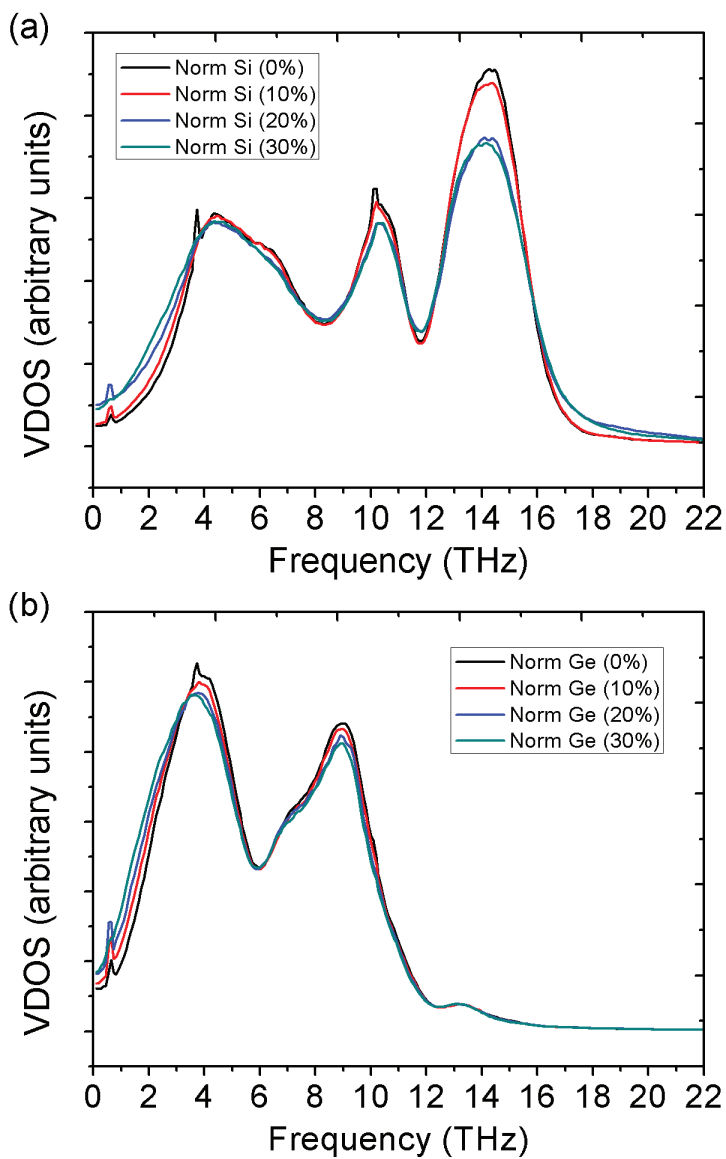
Figure 7: Vibrational density of states of interior (a) Si and (b) Ge atoms with different surface roughness.
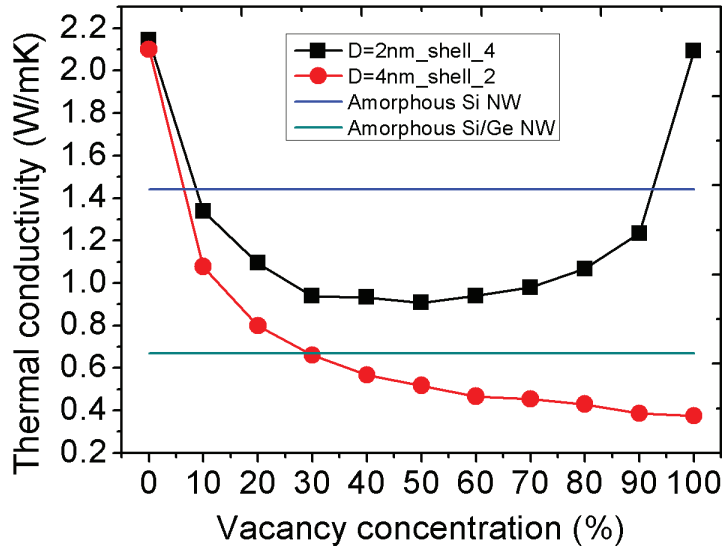
Figure 8: The thermal conductivity of Si/Ge SLNTs as a function of surface vacancy concentration (surface roughness). The blue and cyan horizontal lines represent the thermal conductivity of amorphous Si and $Si_{0.5}Ge_{0.5}$ nanowire, respectively.

4   Conclusions

In conclusion, we have investigated the thermal transport in Si/Ge superlattice nanotubes by performing nonequilibrium molecular dynamics simulations. The results show that the thermal conductivity of Si/Ge superlattice nanotubes depends nonmonotonically on periodic length. As the wall thickness increases, the thermal conductivity of Si/Ge superlattice nanotubes increases due to the increasing of relative contribution of longitudinal modes. However, the thermal conductivity of Si/Ge superlattice nanotubes is not sensitive to the inner diameters due to the strong surface scattering at thin wall thickness. In addition, we found that introducing roughness onto the superlattice nanotubes surface can destroy the phonon tunneling in superlattice nanotubes, which results that the thermal conductivity can be further reduced. By quantifying relative contribution from phonon polarizations and calculating the vibrational density of states of phonons, we found that as the surface roughness increases, the transverse modes are enhanced, which leads to the reduction of thermal conductivity, since the transverse modes have lower frequency and lower phonon group velocities as compared with longitudinal modes. Upon introducing surface roughness, a nonmonotonic dependence of the thermal

conductivity of Si/Ge superlattice nanotubes with thicker wall thickness is found. In contrast, the thermal conductivity of Si/Ge superlattice nanotubes with thinner wall thickness depends monotonically on the surface roughness. Our atomistic simulation results show that, by introducing roughness onto the superlattice nanotubes surface, the thermal conductivity of the Si/Ge superlattice nanotubes can even surpass the alloy limit. The above findings suggest that, by optimizing the periodic length and the nanotube cross-sectional area and introducing appropriate surface roughness, the superlattice nanotubes can be good candidates for high performance thermoelectrics.

References

Chakraborty, S.; Kleint, A.; Heinrich, A.; Schneider, C. M.; Schumann, J.; Falke, M.; Teichert, S. (2003): Thermal conductivity in strain symmetrized Si/Ge superlattices on Si(111). *Appl. Phys. Lett.*, vol. 83, no. 20, pp. 4184-4186.

Chen, J.; Zhang, G.; Li, B. (2010): Remarkable Reduction of Thermal Conductivity in Silicon Nanotubes. *Nano Lett.*, vol. 10, no. 10, pp. 3978-3983.

Cui, Y.; Lieber, C. M. (2001): Functional nanoscale electronic devices assembled using silicon nanowire building blocks. *Science*, vol. 291, no. 5505, pp. 851–853.

Donadio, D.; Galli, G. (2009): Atomistic Simulations of Heat Transport in Silicon Nanowires. *Phys. Rev. Lett.*, vol. 102, no. 19, pp. 195901.

Donadio, D.; Galli, G. (2010): Temperature Dependence of the Thermal Conductivity of Thin Silicon Nanowires. *Nano Lett.*, vol. 10, no. 3, pp. 847–851.

Guiksen, M. S.; Lauhon, L. J.; Wang, J.; Smith, D. C.; Lieber, C. M. (2002): Growth of nanowire superlattice structures for nanoscale photonics and electronics. *Nature*, vol. 415,no. 6872, pp. 617–620.

Haskins, J. B.; Kinaci, A.; Cagin, T. (2011): Thermal conductivity of Si-Ge quantum dot superlattices. *Nanotechnology*, vol. 22, no. 15, pp. 155701.

He, Y.; Donadio, D.; Galli, G. (2011): Morphology and Temperature Dependence

of the Thermal Conductivity of Nanoporous SiGe. *Nano Lett.*, vol. 11, no. 9, pp. 3608–3611.

Hochbaum, A. I.; Chen, R.; Delgado, R. D.; Liang, W.; Garnett, E. C.; Najarian, M.; Majumdar, A.; Yang, P. (2008): Enhanced thermoelectric performance of rough silicon nanowires. *Nature*, vol. 451, no. 7175, pp. 163–U5.

Holmes, J. D.; Johnston, K. P.; Doty, R. C.; Korgel, B. A. (2000): Control of thickness and orientation of solution-grown silicon nanowires. *Science*, vol. 287, no. 5457, pp. 1471–1473.

Hoover, W. G. (1985): Canonocal dynamics-equilibrium phase-space distributions. *Phys. Rev. A*, vol. 31, no. 3, pp. 1695-1697.

Huang, Y.; Duan, X.; Cui, Y.; Lauhon, L. J.; Kim, K.; Lieber, C. M. (2001): Logic gates and computation from assembled nanowire building blocks. *Science*, vol. 294, no. 5545, pp. 1313–1317.

Hu, M.; Giapis, K. P.; Goicochea, J. V.; Zhang, X.; Poulikakos, D. (2011): Significant Reduction of Thermal Conductivity in Si/Ge Core-Shell Nanowires. *Nano Lett.*, vol. 11, no. 2, pp. 618-623.

Hu, M.; Zhang, X.; Giapis, K. P.; Poulikakos, D. (2011): Thermal conductivity reduction in core-shell nanowires. *Phys. Rev. B*, vol. 84, no. 8, pp. 085442.

Hu, M.; Poulikakos, D. (2012): Si/Ge Superlattice Nanowires with Ultralow Thermal Conductivity. *Nano Lett.*, vol. 12, no. 11, pp. 5487–5494.

Hu, M.; Zhang, X.; Poulikakos, D. (2013): Anomalous thermal response of silicene to uniaxial stretching. *Phys. Rev. B*, vol. 87, no. 19, pp. 195417.

Kikkawa, J.; Ohno, Y.; Takeda, S. (2005): Growth rate of silicon nanowires. *Appl. Phys. Lett.,* vol. 86, no. 12, pp. 123109.

Lauhon, L. J.; Gudiksen, M. S.; Wang, C. L.; Lieber, C. M. (2002): Epitaxial core-shell and core-multishell nanowire heterostructures. *Nature*, vol. 420, no. 6911, pp. 57–61.

Li, D.; Wu, Y.; Fan, R.; Yang, P.; Majumdar, A. (2003): Thermal conductivity of Si/SiGe superlattice nanowires. *Appl. Phys. Lett.*, vol. 83, no. 15, pp. 3186–3188.

Lieber, C. M. (2002): Nanowire superlattices. *Nano Lett.*, vol. 2, no. 2, pp. 81–82.

Lin, K.; Strachan, A. (2013): Thermal transport in SiGe superlattice thin films and nanowires: Effects of specimen and periodic lengths. *Phys. Rev. B*, vol. 87, no.11, pp. 115302.

Liu, C. K.; Yu, C. K.; Chien, H. C.; Kuo, S. L.; Hsu, C. Y.; Dai, M. J.; Luo, G. L.; Huang, S. C.; Huang, M. J. (2008): Thermal conductivity of Si/SiGe superlattice films. *J. Appl. Phys.*, vol. 104, no. 11, pp. 144301.

Liu, L.; Chen, X. (2010): Effect of surface roughness on thermal conductivity of silicon nanowires. *J Appl. Phys.*, vol. 107, no. 3, pp. 033501.

Morales, A. M.; Lieber, C. M. (1998): A laser ablation method for the synthesis of crystalline semiconductor nanowires. *Science*, vol. 279, no. 5348, pp. 208–211.

Muller-Plathe, F. J. (1997): A simple nonequilibrium molecular dynamics method for calculation the thermal conductivity. *J. Chem. Phys.*, vol. 106, no. 14, pp. 6082–6085.

Plimpton, S. (1995): Fast parallel algorithms for short-range molecular-dynamics. *J. Comput. Phys.*, vol. 117, no. 1, pp. 1-19.

Simkin, M. V.; Mahan, G. D. (2000): Minimum thermal conductivity of superlattices. *Phys. Rev. Lett.*, vol. 84, no. 5, pp. 927-930.

Venkatasubramanian, R. (2000): Lattice thermal conductivity reduction and phonon localizationlike behavior in superlattice structures. *Phys. Rev. B*, vol. 61, no. 4, pp. 3091-3097.

Wang, N.; Zhang, Y. F.; Tang, Y. H.; Lee, C. S.; Lee, S. T. (1998): SiO2-enhanced synthesis of Si nanowires by laser ablation. *Appl. Phys. Lett.,* vol. 73, no. 26, pp. 3902–3904.

Wu, Y.; Cui, Y.; Huynh, L.; Barrelet, C. J.; Bell, D. C.; Lieber, C. M. (2004): Controlled growth and structures of molecular-scale silicon nanowires. *Nano Lett.*, vol. 4, no.3, pp. 433–436.

Zhang, Y. F.; Tang, Y. H.; Wang, N.; Yu, D. P.; Lee, C. S.; Bello, I.; Lee, S. T. (1998): Silicon nanowires prepared by laser ablation at high temperature. *Appl. Phys. Lett.,* vol. 72, no. 15, pp. 1835–1837.

Zhang, X.; Hu, M.; Giapis, K. P.; Poulikakos, D. (2012): Schemes for and Mechanisms of Reduction in Thermal Conductivity in Nanostructured Thermoelectrics. *ASME J. Heat Transfer*, vol. 134, no. 10, pp. 102042.

Zhang, X.; Hu, M.; Tang, D. (2013): Thermal rectification at silicon/horizontally aligned carbon nanotube interfaces. *J. Appl. Phys.*, vol. 113, no. 19, pp. 194307.

Zheng, G. F.; Lu, W.; Jin, S.; Lieber, C. M. (2004): Synthesis and fabrication of high-performance n-type silicon nanowire transistors. *Adv. Mater.*, vol, 16, no. 21, pp. 1890.